This is a pre-print of an article published in
Journal of Advanced Microscopy Research.
The final authenticated version is available online at:
https://doi.org/10.1166/jamr.2018.1403

INFLUENCE OF SUBSTRATE MATERIAL ON THE MICROSTRUCTURE OF Cu_2ZnSnS_4 THIN FILMS

Yauheni V. Asakovich*; Simon A. Bashkirov; Alena V. Stanchik; Valery F. Gremenok; Raimondas Giraitis; Mikhail S. Tivanov; Gennady F. Novikov; Vladimir V. Rakitin; Uladzimir S. Hekkel.

*E-mail: eugene.osakovich@gmail.com, Tel: +375296526300, Mail: 220072 P. Brovki 19, Minsk, Belarus.

Abstract: Cu_2ZnSnS_4 (CZTS) thin films were synthesized from subsequently electrochemically deposited Cu/Sn/Zn metal precursors on Mo, Ti and Ta foil substrates by sulfurization at 450 °C for 1 h. Polycrystalline CZTS films with the kesterite structure were formed on each substrate. The lattice parameters of CZTS in films are a = 5.414 ± 0.003 Å, c = 10.85 ± 0.02 Å for Mo substrate, a = 5.415 ± 0.001 Å, c = 10.78 ± 0.01 Å for Ti substrate and a = 5.420 ± 0.003 Å, c = 10.84 ± 0.01 Å for Ta substrate. The CZTS have an average grain sizes of about 53, 80 and 68 nm for Mo, Ti and Ta substrate respectively. The films showed two types of crystallites corresponding to CZTS and CuS phases. The films exhibit Cu-enrichment and the presence of CuS and ZnS secondary phases. Binary sulfides MoS_2 and TaS_2 were found in the films deposited on Mo and Ta substrates respectively.

Keywords: Cu_2ZnSnS_4; CZTS; thin films; microstructure; electrochemical deposition; sulfurization; foil substrate.

1. INTRODUCTION

Among the multi-component metal chalcogenides, Cu_2ZnSnS_4 (CZTS) rises increasing interest as a promising light-absorbing material to substitute $Cu(In,Ga)(S,Se)_2$ (CIGS) and CdTe in thin films solar cells. Despite the proven efficiency of the latter materials, their share in the global energy market remains low due to the rarity and high costs of In and Ga, as well as the toxicity of Cd. As an alternative, CZTS has been designed to overcome the problems of its predecessors. CZTS is a I_2-II-IV-VI_4 quaternary p-type semiconductor material with a kesterite/stannite structure. CZTS posses direct band gap of about 1.5 eV and a large absorption coefficient ($> 10^4$ cm^{-1}) in the visible spectral range[1,2,3]. Each component of CZTS is earth-abundant and harmless to the environment in the used amounts. The latest reported conversion efficiency record for the CZTS-based solar cell is 11% [4] with a theoretical limit of about 32% [5].

Amid the different vacuum and non-vacuum methods of synthesizing CZTS films the most promising one, due to its low cost and scalability, is electrochemical deposition of metallic Cu-Sn-Zn precursors followed by their annealing in sulfur-containing media (sulfurization). The highest conversion efficiency for CZTS-based solar cells prepared from electrochemically deposited metallic precursors is 8,3% [6]. However, the effect of secondary phases, small stoichiometry deviations and surface morphology features of the CZTS films on their functionality as the absorbing layers in solar cells still requires the further systematic study.

To obtain the efficient thin film solar cell, it is very important to apply the optimal substrate and back contact materials. The general requirements include the ohmic type of the contact and its chemical stability in the sulfurization conditions. The most commonly used substrate material for both CIGS and CZTS thin film solar cells is Mo-coated glass. However, a number of metals including Ta, Ti, and others meet the requirements mentioned above. Moreover, the use of flexible substrates, such as metal foils, opens additional practical advantages. Previously, we reported the influence of the substrate material on the microstructure of $Cu_2ZnSnSe_4$ (CZTSe)[7]. This paper

presents the investigation of substrate material effect on the microstructure of CZTS thin films obtained by sulfurization of electrochemically deposited Cu/Sn/Zn stack precursors.

2. EXPERIMENTAL DETAILS

Flexible 0.05 mm thick Mo, Ti and Ta foil substrates were mechanically polished, cleaned with ethanol, rinsed with deionized water. The CZTS thin films were fabricated by a two-step process. At the first step, the metal precursors were deposited in the subsequence of layers as Cu/Sn/Zn by electrochemical deposition in a two-electrode cell in galvanostatic mode. The plates of high purity (99.999%) copper, tin, and zinc were used as anodes for the respective metal layers deposition. The electrolytes were prepared based on the sulfates solutions of the respective metals. At the second step, the samples were sulfurized at 450°C in the two-zone tube furnace in graphite block. Nitrogen was used as a carrier gas with N_2+S_2 pressure maintained about 0.8 mbar. The 30°C/min heating rate was used to reach 300°C and then changed to 5°C/ min to achieve the desired temperature of 450°C. The sulfurization process lasted 1 hour and then the samples were naturally cooled in the furnace to room temperature.

The phase composition of the materials was analyzed by x-ray diffraction (XRD) using D8 Advance (Bruker AXS) with CuK_α radiation (λ = 1.5418 Å). Phase analysis was carried out using Crystallography Open Database (COD). The lattice parameters, grain sizes and microstrain values for CZTS, CuS phases and substrate material were evaluated using «Material Analysis Using Diffraction (MAUD)» software package[8] based on the full-profile analysis of X-ray patterns by Rietveld method. To confirm the phase analysis of the materials, room-temperature Raman measurements using Nanofinder HE (LOTIS TII) confocal Raman spectrometer with a spectral resolution better than 3 cm^{-1} proceeded. The Raman spectra were excited with a solid laser emitting at a wavelength of 532 nm with an optical power of 60 and 200 μW to analyze the composition in detail both on the surface and in the deeper layers. The diameter of the laser beam at the sample surface was 0.6–0.7 μm. The surface morphology of CZTS films was examined by scanning electron microscopy (SEM) using Helios Nanolab 650 Electron Microscope (FEI Company) with

Oxford Instruments Spectrometer to determine the elemental composition of the films by energy dispersive X-ray microanalysis (EDX).

3. RESULTS AND DISCUSSION

Fig. 1 shows the X-ray diffraction patterns of as-synthesized CZTS thin films on Mo, Ti and Ta substrates. The lattice parameters, grain sizes and microstrain values for CZTS, are presented in Table 1. The lattice parameters of CZTS and CuS phases in films are close to the values for bulk material[9,10]. The lattice parameters for substrate materials are a = 3.1476 ± 0.0001 Å for Mo, a = 2.9443 ± 0.0004 Å, c = 4.6759 ± 0.0004 Å for Ti and a = 3.3072 ± 0.0001 Å for Ta. An average grain size is about 352, 73 and 52 nm for Mo, Ti and Ta substrates respectively. According to the results, polycrystalline CZTS films (tetragonal, space group I-42m) with kesterite structure were formed on each substrate showing reflections at 28° (112), 33° (200, 004), 37°, 48° (220, 204), 56° (312), 69° (400, 008) and 77° (332, 316), but with different grain sizes (Table 1). Such a difference can be explained by the deviations in the stoichiometry of the films, that lead to the formation of secondary phases that cause residual strains and interfere with the normal growth of the CZTS. As expected, typical peaks for Mo (cubic, space group Im-3m), Ti (hexagonal, space group P63/mmc) and Ta (cubic, space group Im-3m) also presented in XRD pattern. However, there is a significant number of peaks in the XRD pattern that can be identified as the CuS (hexagonal, space group P63/mmc) secondary phase. Despite the fact that low-intensity peaks (reflections at 2θ=31°) in the patterns may correspond to the ZnS secondary phase since the sphalerite ZnS (cubic, space group F-43m) has reflexes overlapping with CZTS, it cannot be clearly observed by XRD. It should be noted that in the patterns of CZTS on Mo substrate an unidentified peak was observed (reflection at 2θ=43°) which is identified as the reflexion from the Sn_3S_4 phase in other work[11].

Raman scattering measurements were carried out to confirm the phase composition of the materials. Raman spectra (Fig. 2) confirm the presence of CZTS and CuS phases in the samples. The spectra show two dominant peaks about 335 cm^{-1} and 287 cm^{-1} which assign by many authors as the characteristic peaks for CZTS with kesterite structure[12,13]. The spectra also show weaker

contributions at 83, 98, 165, 252, 269, 311 and 364 cm^{-1} that are attributed to E and B symmetry modes [14]. The peaks at 68, 139 and 475 cm^{-1} indicate the presence of a CuS in the samples. Also, binary sulfides phases such as MoS_2 with the peak at 408 cm^{-1} (Fig. 2.1) and TaS_2 with the peak at 405 cm^{-1} (Fig. 2.3) are present on the spectra, which were not detected by XRD. The absence of TiS_2 phase is explained by the fact that the sulfurization temperature was lower than the temperature of the formation (550°C) of this phase[15]. Used optical power of 200 μW allowed to detect the presence of binary sulfides which are located in deeper layers of the material and a low-intensity peak at 667 cm^{-1} refers to the ZnS secondary phase as shown in other work[16].

According to the EDX measurements (Table 2), the samples are Cu-rich which leads to the formation of the CuS secondary phase shown by XRD and Raman measurements. It is important to mention that sample with Mo substrate contains a very small amount of Sn which is probably related to tin evaporation during the sulfurization process[3]. The removal of tin from the material composition during sulfurization process of precursors without pre-annealing can be ascribed to the formation of SnS volatile compound. To avoid such tin loss, the pre-annealing of the precursors should be used in the future[17]. Also, it is proposed to carry out a sulfurization process with the addition of Sn powder in the reaction chamber[18].

SEM images of the CZTS films surface is presented in Fig. 3 and 4. The surface of each sample shows significant inhomogeneity. In the SEM images of each sample, it is possible to determine two types of crystallites. The small ones have a size of about 100 nm or less and due to their symmetry can be identified as CZTS crystallites. The large ones reach the size of several micrometers and have been identified as CuS crystallites[13]. The surface of the film deposited on Mo substrate (Fig. 4.1) is almost half covered with crystallites, which we identified as CuS and slightly less intensive on Ta (Fig. 4.3). Unlike the other two, on the Ti substrate, CuS crystallites are present only in certain areas, which can be seen in the Fig. 4.2. These observations are well correlated with the data obtained by EDX measurements. This kind of morphology can be explained by the multiphaseous nature of the films. The Cu atoms seem to diffuse to the outer surface of the film

during the sulfurization that can be attributed to the high reactivity between Cu and S. The CuS crystallites located on the surface of the film can be effectively removed by etching with KCN[19,20].

4. CONCLUSION

In this work, the Cu_2ZnSnS_4 thin films with kesterite structure were fabricated and the influence of substrate material on the microstructure of the films was studied. The lattice parameters for CZTS phase are $a = 5.414 \pm 0.003$ Å, $c = 10.85 \pm 0.02$ Å for Mo substrate, $a = 5.415 \pm 0.001$ Å, $c = 10.78 \pm 0.01$ Å for Ti substrate and $a = 5.420 \pm 0.003$ Å, $c = 10.84 \pm 0.01$ Å for Ta substrate. The Cu enrichment of the thin films decreases depending on the used substrate material: from Mo to Ta and Ti, respectively, leading to the less formation of CuS secondary phase. The tin loss may be explained by its evaporation during the sulfurization process. The CuS, as can be seen on SEM images, is located on the surface and, thus, it can be removed by etching the films with KCN in the further technological steps. The CZTS crystallizes in small-sized crystallites with an average size of about 53, 80 and 68 nm for Mo, Ti and Ta substrate respectively. The biggest values of grain size are observed for the films with the lowest deviation from stoichiometry. The difference in the average size can be explained by the deviations in the stoichiometry of the films leading to the formation of secondary phases that cause residual strains and affect the normal CZTS growth. The results of this study will be used for further development of the technology for production of CZTS thin films.

ACKNOWLEDGEMENTS

This study was financially supported by Belarussian Republican Foundation for Fundamental Research (F17RM-089), the Russian Foundation for Basic Research (grant no.17-58-04039) and the Belarusian State Programme for Research «Physical material science, new materials, and technologies» (MATTEX 1.06).

REFERENCES

1. V.V. Rakitin, G.F. Novikov. Third-generation solar cells based on quaternary copper compounds with the kesterite-type structure. Russian Chemical Reviews. 86, 99 (2017).
2. H.Katagiri, M.Nishimura, T. Onozawa, S.Maruyama, M. Fujita, T. Sega, T.Watanabe, Editors. Rare-metal free thin solar cell. Proceedings of the Power Conversion Conference – Nagaoka'97, (1997) August 6; Nagaoka, Japan.
3. S.A. Bashkirov, R. Kondrotas, V.F. Gremenok, R. Juškėnas, I.I. Tyukhov. $Cu_2ZnSn(S,Se)_4$ thin films for application in third generation solar cells, International Scientific Journal for Alternative Energy and Ecology. 15-18, 31 (2016).
4. K. Sun, C. Yan, F. Liu, J. Huang, F. Zhou, J.A. Stride, M. Green, X. Hao. Over 9% efficient kesterite Cu_2ZnSnS_4 solar cell fabricated by using Zn_{1-x} Cd_xS Buffer Layer. Adv. Energy Mater. 6, 1600049 (2016).
5. M.P. Paranthaman, W. Wong-Ng, R.N. Bhattacharya, Semiconductor Materials for Solar Photovoltaic Cells, Springer International Publishing, Switzerland (2016).
6. H. Xin, J.K. Katahara, I. L. Braly, H. W. Hillhouse. 8% Efficient $Cu_2ZnSn(S,Se)_4$ Solar Cells from Redox Equilibrated Simple Precursors in DMSO. Adv. Energy Mater. 4, 1301823 (2014).
7. A.V. Stanchik, V. F. Gremenok, S. A. Bashkirov, M. S. Tivanov, R. L. Juskenas, G. F. Novikov, R. Giraitis, A. M. Saad. Microstructure and Raman scattering of $Cu_2ZnSnSe_4$ thin films deposited onto flexible metal substrates. Semiconductors. 52, 215 (2018).
8. MAUD (Material Analysis Using Diffraction): a user-friendly Java program for Rietveld Texture Analysis and more. L. Lutterotti, S. Matthies and H.R. Wenk. Proceeding of the Twelfth International Conference on Textures of Materials (ICOTOM-12). 1, 1599 (1999).
9. P. Bonazzi, L. Bindi, G. P. Bernardini, S. Menchetti. A model for the mechanism of incorporation of Cu, Fe, and Zn in the stannite - kesterite series, Cu_2FeSnS_4 - Cu_2ZnSnS_4. The Canadian Mineralogist, Canada (2003), Vol. 41, pp. 639-647.
10. H. T. Evans, J. A. Konnert. Crystal structure refinement of covellite. American Mineralogist. 61, 996 (1976).

11. Tulshi Shiyani, Dhyey Raval, Malkeshkumar Pate l, Indrajit Mukhopadhyay, Abhijit Ray. Effect of initial bath condition and post-annealing on co-electrodeposition of Cu_2ZnSnS_4. Materials Chemistry and Physics. 171, 63 (2016).
12. A. Lafond, L. Choubrac, C. Guillot-Deudon, P. Fertey, M. Evain, S. Jobic. X-ray resonant single-crystal diffraction technique, a powerful tool to investigate the kesterite structure of the photovoltaic Cu_2ZnSnS_4 compound. Acta Cryst. Section B. 70, 390 (2014).
13. P.A. Fernandes, P.M.P. Salome, A.F. Gunha. Growth and Raman scattering characterization of Cu_2ZnSnS_4 thin films. Thin Solid Films. 517, 2519 (2008).
14. X. Fontané, V. Izquierdo-Roca, E. Saucedo, S. Schorr, V.O. Yukhymchuk, M.Ya. Valakh, A. Pérez-Rodríguez, J.R. Morante. Vibrational properties of stannite and kesterite type compounds: Raman scattering analysis of $Cu_2(Fe,Zn)SnS_4$. Journal of Alloys and Compounds. 539, 190 (2012).
15. M. J. Mckelvy, W. S. Claunsinger, in Inorganic Syntheses: Nonmolecular solids, Edited D. W. Murphy, L. V. Interrante, John Wiley Sons Inc., New York (1995) Vol. 30, pp. 28–32.
16. M. Dimitrievska, A. Fairbrother, X. Fontané, T. Jawhari, V. Izquierdo-Roca1, E. Saucedo, A. Pérez-Rodríguez. Multiwavelength excitation Raman scattering study of polycrystalline kesterite Cu_2ZnSnS_4 thin films. Appl. Phys. Lett. 104, 021901 (2014).
17. R. Juškėnas, R. Giraitis, S. Kanapeckaitė, V. Karpavičienė, Z. Mockus, G. Niaura, V. Pakštas, A. Selskienė. A two-step approach for electrochemical deposition of Cu-Zn-Sn and Se precursors for CZTSe solar cells. Sol. Energy Mater. Sol. Cells. 101, 277 (2012).
18. A. Redinger, D. M. Berg, P. J. Dale, S. Siebentritt. The consequences of kesterite equilibria for efficient solar cells. J. Am. Chem. Soc. 133, 3320 (2011).
19. K. Timmo, M. Altosaar, J. Raudoja, M. Grossberg, M. Danilson, O. Volobujeva, E. Mellikov, Editors. Chemical etching of $Cu_2ZnSn(S,Se)_4$ monograin powder. Proceedings of the 35th IEEE Photovoltaic Specialists Conference, (2010) June 20-25; Honolulu, Hawaii.

20. Kee Doo Lee, Se-Won Seo, Doh-Kwon Lee, Honggon Kim, Jeung-Hyun Jeong, Min Jae Ko, BongSoo Kim, Dong Hwan Kim, Jin Young Kim. Preparation of Cu_2ZnSnS_4 thin films via electrochemical deposition and rapid thermal annealing. Thin Solid Films. 546, 294 (2013).

List of figures

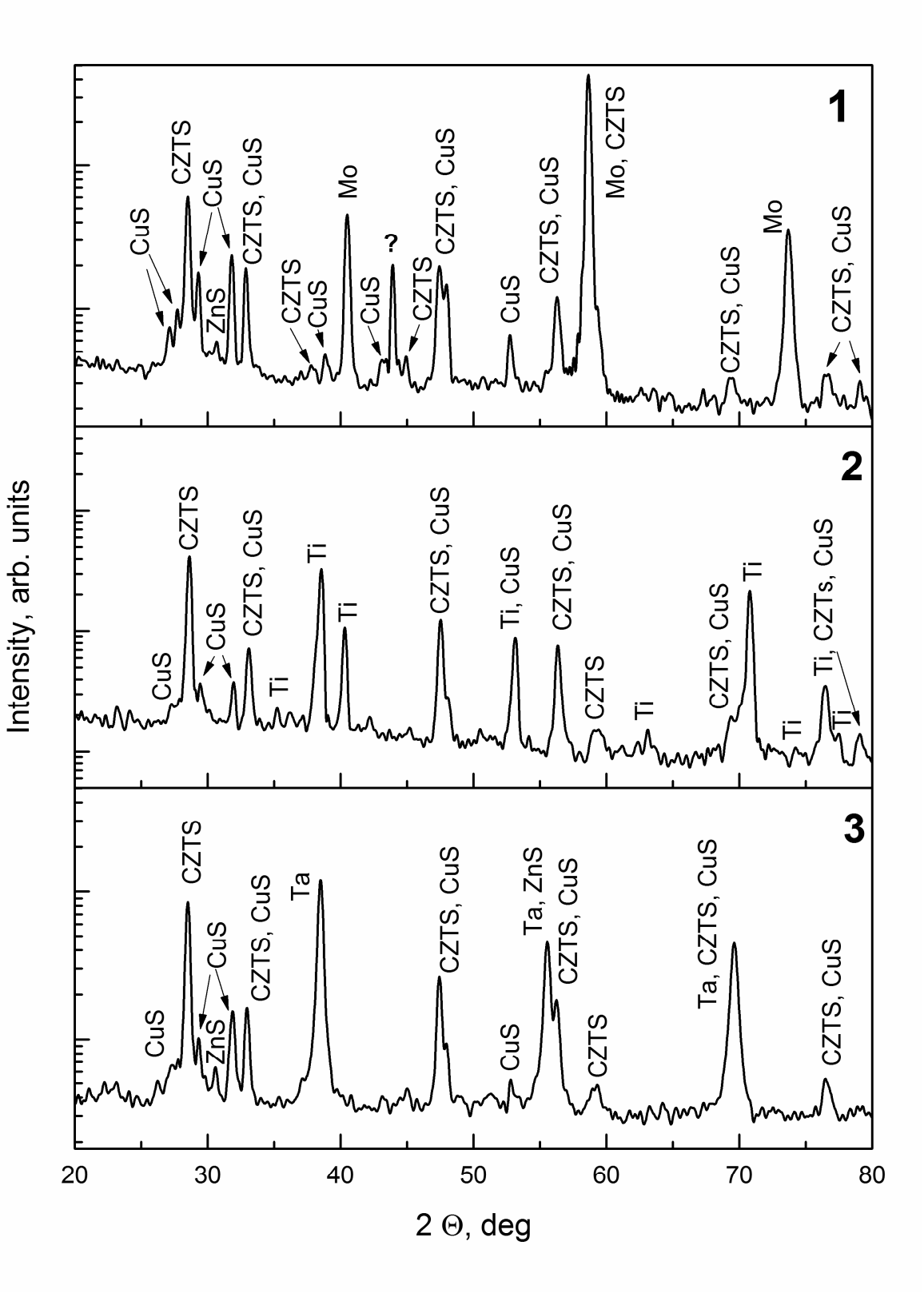
Intensity, arb. units
2 Θ, deg
20
30
40
50
60
70
80
1
2
3
CuS
CZTS
ZnS
CZTS, CuS
Mo
?
Mo, CZTS
Ti
Ti, CuS
Ti, CZTs, CuS
Ta
Ta, ZnS
Ta, CZTS, CuS

Fig. 1.

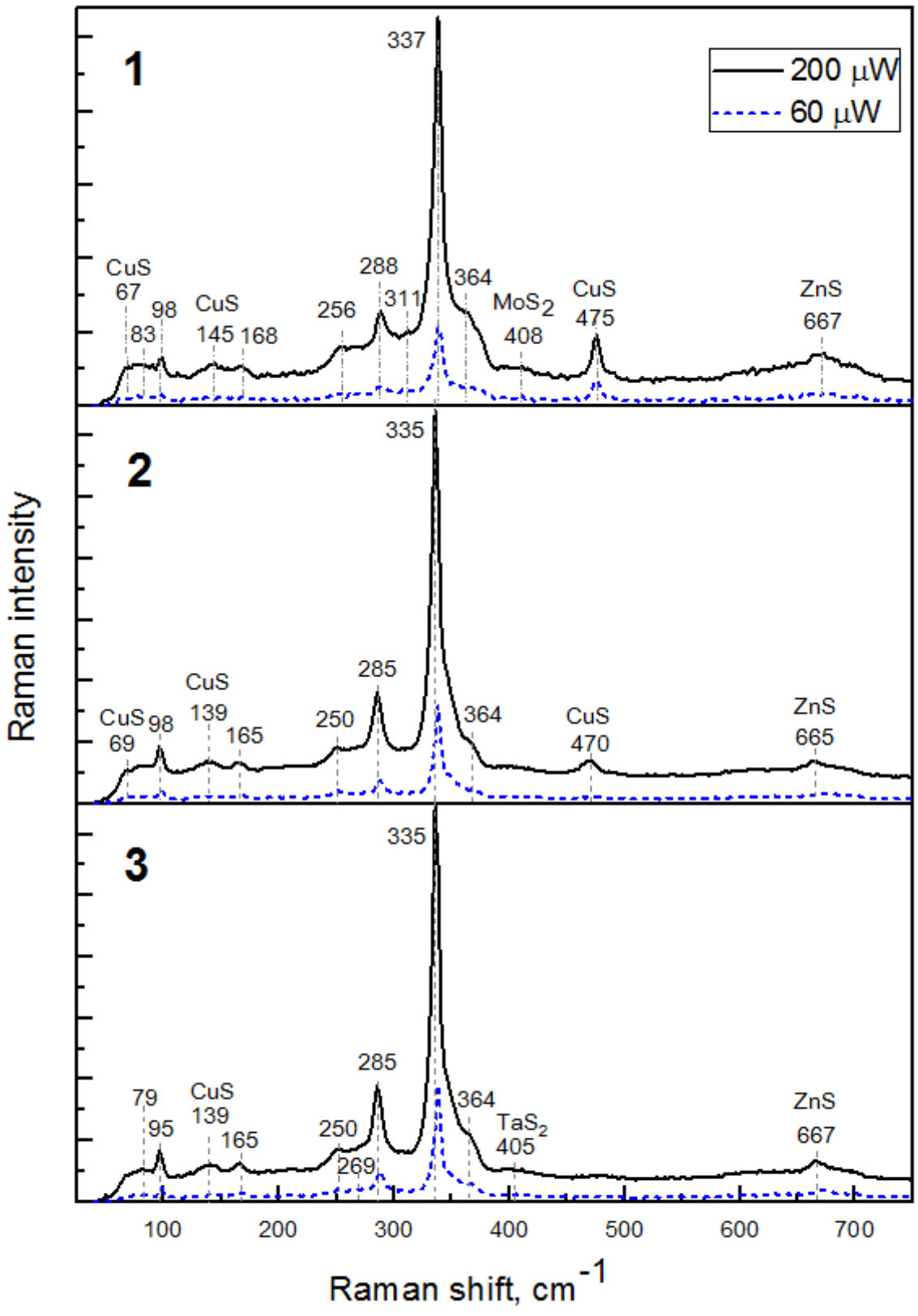
1
2
3
200 μW
60 μW
337
288
311
364
256
CuS
67
98
83
CuS
145
168
MoS2
408
CuS
475
ZnS
667
335
285
CuS
139
165
250
CuS
69
98
364
CuS
470
ZnS
665
335
285
79
95
CuS
139
165
250
269
364
TaS2
405
ZnS
667
Raman intensity
100
200
300
400
500
600
700
Raman shift, cm-1

Fig. 2.

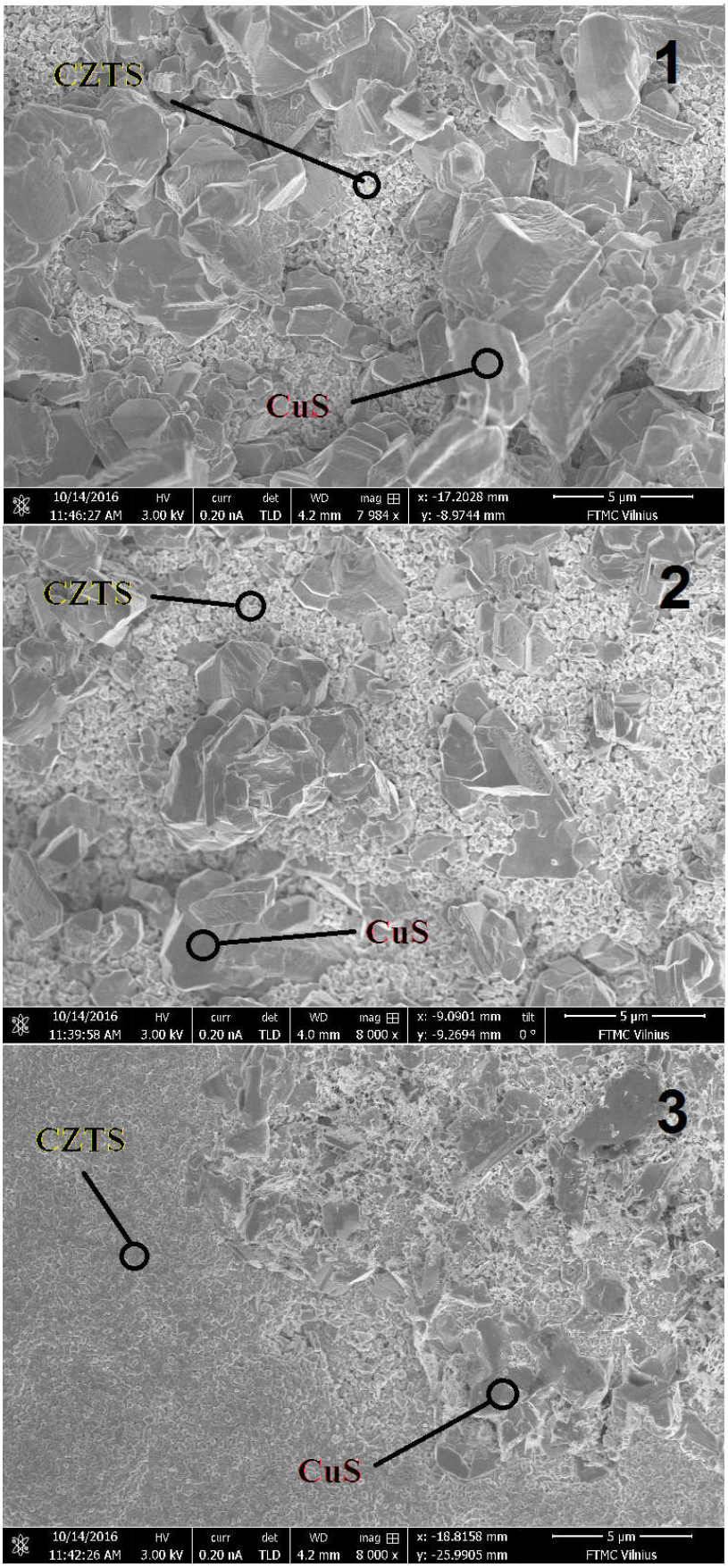
CZTS
CuS
1
10/14/2016 11:46:27 AM HV 3.00 kV curr 0.20 nA det TLD WD 4.2 mm mag 7 984 x x: -17.2028 mm y: -8.9744 mm 5 µm FTMC Vilnius
CZTS
CuS
2
10/14/2016 11:39:58 AM HV 3.00 kV curr 0.20 nA det TLD WD 4.0 mm mag 8 000 x x: -9.0901 mm y: -9.2694 mm tilt 0 ° 5 µm FTMC Vilnius
CZTS
CuS
3
10/14/2016 11:42:26 AM HV 3.00 kV curr 0.20 nA det TLD WD 4.2 mm mag 8 000 x x: -18.8158 mm y: -25.9905 mm 5 µm FTMC Vilnius

Fig. 3.

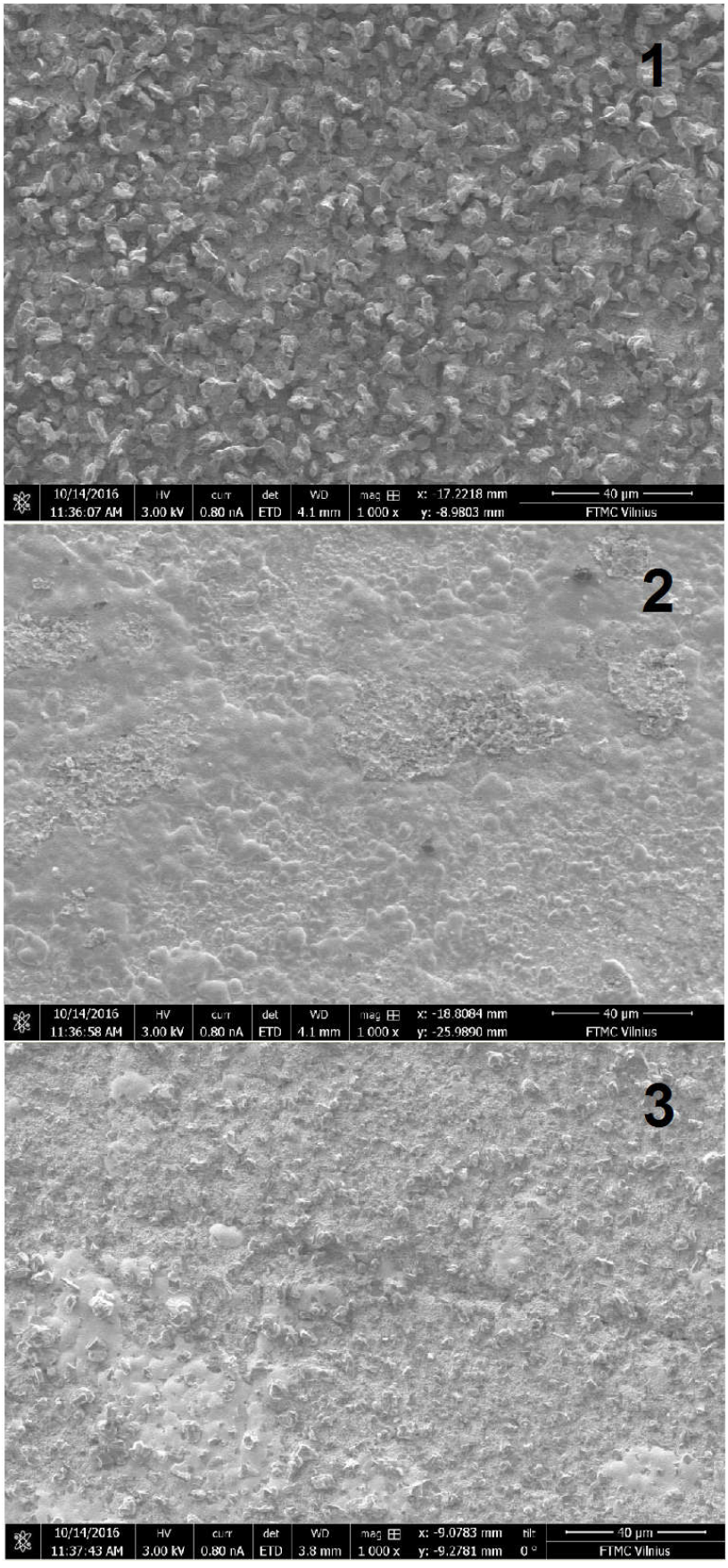
1
10/14/2016
11:36:07 AM
HV
3.00 kV
curr
0.80 nA
det
ETD
WD
4.1 mm
mag
1 000 x
x: -17.2218 mm
y: -8.9803 mm
40 µm
FTMC Vilnius
2
10/14/2016
11:36:58 AM
HV
3.00 kV
curr
0.80 nA
det
ETD
WD
4.1 mm
mag
1 000 x
x: -18.8084 mm
y: -25.9890 mm
40 µm
FTMC Vilnius
3
10/14/2016
11:37:43 AM
HV
3.00 kV
curr
0.80 nA
det
ETD
WD
3.8 mm
mag
1 000 x
x: -9.0783 mm
y: -9.2781 mm
tilt
0 °
40 µm
FTMC Vilnius

Fig. 4.

Table 1. The XRD measurements of CZTS and secondary phases (a, c – lattice parameters, D – grain size, ε – microstrain value)

Substrate \ Phase		CZTS	CuS
Mo	*a*, Å	5.414 ± 0.003	3.789 ± 0.001
	c, Å	10.85 ± 0.02	16.349 ± 0.004
	D, nm	53 ± 3	127 ± 20
	ε, 10^{-3}	1.8 ± 0.2	2.0 ± 0.2
Ti	*a*, Å	5.415 ± 0.001	3.776 ± 0.002
	c, Å	10.78 ± 0.01	16.242 ± 0.017
	D, nm	80 ± 5	98 ± 60
	ε, 10^{-3}	2.1 ± 0.2	2.0 ± 0.9
Ta	*a*, Å	5.420 ± 0.003	3.786 ± 0.001
	c, Å	10.84 ± 0.01	16.328 ± 0.006
	D, nm	68 ± 2	93 ± 20
	ε, 10^{-3}	1.9 ± 0.1	2.4 ± 0.3
Ref.	*a*, Å	5.434	3.7938
	c, Å	10.856	16.341
	№	9	10

Table 2. The at. % ratio of the CZTS components

Substrate	Composition ratio, at. %						
	Cu	Sn	Zn	S	Cu/(Sn+Zn)	Zn/Sn	(Cu+Sn+Zn)/S
Mo	30.9	3.6	17.6	47.9	1.46	4.89	1.09
Ti	25.9	11.3	10.6	52.2	1.18	0.94	0.92
Ta	28.7	7.8	13.1	50.4	1.37	1.68	0.98